



The 2015 super-active state of recurrent nova T CrB and the long term evolution after the 1946 outburst[☆]



Ulisse Munari^{a,*}, Sergio Dallaporta^b, Giulio Cherini^b

^aINAF Astronomical Observatory of Padova, via dell'Osservatorio 8, 36012 Asiago (VI), Italy

^bANS Collaboration, c/o Astronomical Observatory, 36012 Asiago (VI), Italy

HIGHLIGHTS

- In 2015 T CrB has entered a phase of unprecedented high activity.
- Similar to what the star underwent in 1938, a few years before its 1946 nova outburst.
- High ionization conditions, [NeV], OIV and a strong HeII in emission.
- Wind of the M3III companion almost fully ionized, enhanced irradiation of its side facing the WD.
- Disappearance of the orbital modulation from B-band lightcurve, now fully dominated by nebular emission.

ARTICLE INFO

Article history:

Received 1 January 2016

Accepted 18 January 2016

Available online 1 February 2016

Keywords:

Novae

Cataclysmic variables

Symbiotic binaries

ABSTRACT

The recurrent nova T CrB has entered in 2015 a phase of unprecedented high activity. To trace something equivalent, it is necessary to go back to 1938, before the last nova eruption in 1946. The 2015 super-active state is characterized by: a large increase in the mean brightness ($\Delta B=0.72$ mag over the underlying secular trend), vanishing of the orbital modulation from the B-band lightcurve, and appearance of strong and high ionization emission lines, on top of a nebular continuum that overwhelms at optical wavelengths the absorption spectrum of the M giant. Among the emission lines, HeII 4686 attains a flux in excess of H γ , the full set of OIII and NIII lines involved in the Bowen fluorescence mechanism are strong and varying in intensity in phase with HeII 4686, and OIV and [NeV] are present. A large increase in the radiation output from the hot source is responsible for a large expansion in the ionized fraction of the M giant wind. The wind is completely ionized in the direction to the observer. A high electron density is supported by the weakness of forbidden lines and by the large amplitude and short time scale of the reprocessing by the nebular material of the highly variable photo-ionization input from the hot source. During the super-active state the nebula is varying to and from ionization-bounded and density-bounded conditions, and the augmented irradiation of the cool giant has changed the spectral type of its side facing the WD from M3III to M2III, i.e. an increase of ~ 80 K in effective temperature.

© 2016 Elsevier B.V. All rights reserved.

1. Introduction

T CrB is one of the few known Galactic recurrent novae (Warner, 1995; Schaefer, 2010), with outbursts recorded in 1866 and 1946. They have been spectacular events, peaking around 2.0 mag (Pettit, 1946), displaying nearly identical lightcurves characterized by an extremely fast rise to maximum and a rapid decline, taking $t_2=3.8$ days to decline by 2 mag (Paine-Gaposchkin, 1957). The spectroscopic evolution (Sanford, 1946; 1949) was – in

modern terms – that of an He/N nova (Williams, 1992), reaching very high ionization conditions as indicated by the presence of strong [FeX] and [FeXIV] coronal lines (Sanford, 1947). Peculiar to T CrB is the presence on both outbursts, of a secondary, fainter and broader maximum ~ 110 days past the primary maximum, which physical nature is still debated (e.g. Webbink, 1976; Cannizzo and Kenyon, 1992; Selvelli et al., 1992; Ruffert et al., 1993).

The donor star in T CrB is an M3III, filling its Roche lobe (Bailey, 1975; Yudin and Munari, 1993), on a 227.55 day orbit (Kenyon and Garcia, 1986; Fekel et al., 2000) around a WD companion (Selvelli et al., 1992; Belczynski and Mikolajewska, 1998). The presence of a cool giant makes T CrB also a member of the class of symbiotic binaries (Allen, 1984; Kenyon, 1986), similarly to the other symbiotic recurrent novae RS Oph, V745 Sco and V3890 Sgr (Munari, 1997).

[☆] Communicated by P.S. Conti.

* Corresponding author. Tel.: +39 424 600033; fax.: +39 424600023.

E-mail address: ulisse.munari@oapd.inaf.it (U. Munari).

Table 1

Our $BVR_C I_C$ photometric observations of T CrB. The full table is available electronically via CDS, a small portion is shown here for guidance on its form and content.

JD (-2,450,000)	UT date	B	Err	V	Err	R_C	Err	I_C	Err	Id
7277.328	2015 09 11.828	11.058	0.011	9.821	0.004	8.839	0.010	7.447	0.005	11
7283.296	2015 09 17.796	11.188	0.009	9.954	0.008	8.973	0.009	7.566	0.006	11
7284.322	2015 09 18.822	11.103	0.009	9.914	0.012	8.930	0.006	7.533	0.006	36
7286.289	2015 09 20.789	11.029	0.008	9.860	0.009	8.917	0.009	7.536	0.012	11
7287.285	2015 09 21.785	10.931	0.011	9.878	0.011	8.875	0.009	7.593	0.013	11
7291.294	2015 09 25.794	10.809	0.008	9.830	0.011	8.914	0.006	7.585	0.008	36
7300.256	2015 10 04.756	10.763	0.012	9.829	0.010	8.877	0.007	7.579	0.006	36
7301.260	2015 10 05.760	10.802	0.010	9.814	0.007	8.888	0.012	7.624	0.007	11

The brightness in quiescence ($V \sim 10$ mag) and the favourable position on the sky (absence of seasonal gaps in the observability from the northern hemisphere), have fostered continued interest and study of T CrB. In quiescence, typical symbiotic binaries display a rich and high ionization emission line spectrum (comprising [NeV], [CaV], [FeVII], H α , and Raman scattered OVI), superimposed to the absorption spectrum of the cool giant, with the nebular continuum veiling in the yellow, and overwhelming in the blue, its molecular absorption bands (Allen, 1984; Munari and Zwitter, 2002; Skopal, 2005). As a symbiotic binary, the optical quiescence spectrum of T CrB is atypical in showing very little else than the M3III absorption spectrum. Most of the time, only a weak emission in H α is noticeable on low resolution spectra (Kenyon, 1986). On rare occasions, a surge in activity causes the optical spectrum of T CrB to show something more typical of symbiotic binaries, e.g. Balmer lines and continuum in emission, and sometimes even the appearance of a weak H α 4686 in emission (Iijima, 1990; Anupama and Prabhu, 1991).

In this paper we report on the super-active conditions displayed by T CrB during 2015 (in the following SACT-2015 for short), conditions never seen before. SACT-2015 appears to be much stronger, both photometrically and spectroscopically, than previous periods of enhanced activity recorded after the 1946 nova outburst.

2. Observations

$BVR_C I_C$ optical photometry of T CrB is regularly obtained since 2006 with ANS Collaboration telescopes N. 11 and 36, located in Italy in Trieste and Cembra, respectively. The star has been observed on 205 nights, from May 11, 2006 to Dec 20, 2015. The operation of ANS Collaboration telescopes is described in detail by Munari et al. (2012) and Munari and Moretti (2012). The same local photometric sequence, calibrated by Henden and Munari (2006) against Landolt equatorial standards, was used at both telescopes on all observing epochs, ensuring a high consistency of the data. The $BVR_C I_C$ photometry of T CrB is given in Table 1, where the quoted uncertainties are the total error budget, which quadratically combines the measurement error on the variable with the error associated to the transformation from the local to the standard photometric system (as defined by the photometric comparison sequence). All measurements were carried out with aperture photometry, the long focal length of the telescopes and the absence of nearby contaminating stars not requiring to revert to PSF-fitting.

Low resolution spectra of T CrB were obtained with the 1.22 m telescope + B&C spectrograph operated in Asiago by the Department of Physics and Astronomy of the University of Padova. The CCD camera is a ANDOR iDus DU440A with a back-illuminated E2V 42-10 sensor, 2048 \times 512 array of 13.5 μ m pixels. It is highly efficient in the blue down to the atmospheric cut-off around 3250 \AA . The spectral dispersion is 2.31 Ang/pix and the spectral resolution is constant at ~ 2.2 pix, with the spectra extending from ~ 3300 to ~ 8050 \AA . The slit width has been kept fixed at 2 arcsec, and the

slit always aligned with the parallactic angle for optimal absolute flux calibration.

High resolution spectra were obtained with the Echelle spectrograph mounted on the 1.82 m Asiago telescope. It is equipped with an EEV CCD47-10 CCD, 1024 \times 1024 array, 13 μ m pixel, covering the interval $\lambda\lambda$ 3600–7300 \AA in 30 orders, at a resolving power of 20,000 and without inter-order wavelength gaps.

3. Photometric evolution during 2006–2015

The 2006–2015 $BVR_C I_C$ lightcurves of T CrB from our CCD observations of Table 1 are plotted on the left panel of Fig. 1. The much brighter state of T CrB in 2015 is evident, with increasing relevance toward shorter wavelengths. On the right panel of Fig. 1, the 2006–2014 data (preceding SACT-2015) are phase plotted against the orbital ephemeris

$$\text{Min}I = 2431933.83 + 227.55 \times E \quad (1)$$

which gives the epochs of primary minima (passages of the M3III companion at inferior conjunction) for the orbital period derived by Kenyon and Garcia (1986) and Fekel et al. (2000). The resulting phased lightcurve is dominated by the well-known ellipsoidal distortion of the M3III giant, first reported by Bailey (1975) at optical wavelengths and by Yudin and Munari (1993) in the infrared. The over-plotted curves are simple fits to guide the eye, in particular to demonstrate that: (a) the amplitude of the ellipsoidal modulation, as given by the fitting curves, is $\Delta B=0.63$, $\Delta V=0.49$, $\Delta R_C=0.42$, and $\Delta I_C=0.34$ mag; (b) the secondary minimum (phase 0.5, WD passing at inferior conjunction) is shallower at shorter wavelengths, a fact due to the irradiation of the cool giant by the hot WD companion; and (c) the dispersion of points around the fitting curves increases toward shorter wavelengths and is well in excess of the small observational errors (cf Table 1). The reason for that is associated with the erratic behavior of accretion phenomena in the system. In fact, a long record of observations document a large amplitude flickering affecting time series observations of T CrB (e.g. Zamanov and Bruch, 1998; Zamanov et al., 2004; Gromadzki et al., 2006; Dobrotka et al., 2010).

The photometric data on T CrB secured during SACT-2015 are not inserted in the right panel of Fig. 1, which only deals with the preceding quiescence. The SACT-2015 data are instead plotted in Fig. 2, against the same ephemeris as used for Fig. 1, from which the polynomial fits are also copied. From Fig. 2 we infer that: (i) the shorter the wavelength, the larger the increase in brightness during SACT-2015: compared with preceding quiescence (as given by the fitting curves in Figs. 1 and 2), the increase is $\Delta B=0.72$, $\Delta V=0.28$, $\Delta R_C=0.21$, and $\Delta I_C=0.09$ mag; (ii) during SACT-2015, the orbital modulation disappears from the B lightcurve, and the depth of secondary minimum (orbital phase 0.5) is reduced in the V and R_C lightcurves; and (iii) contrary to previous high states that did not influence T CrB brightness at longer wavelengths, the effect of SACT-2015 extends well into the far red, with all I_C measurements laying above the polynomial fit to quiescence data. Anticipating

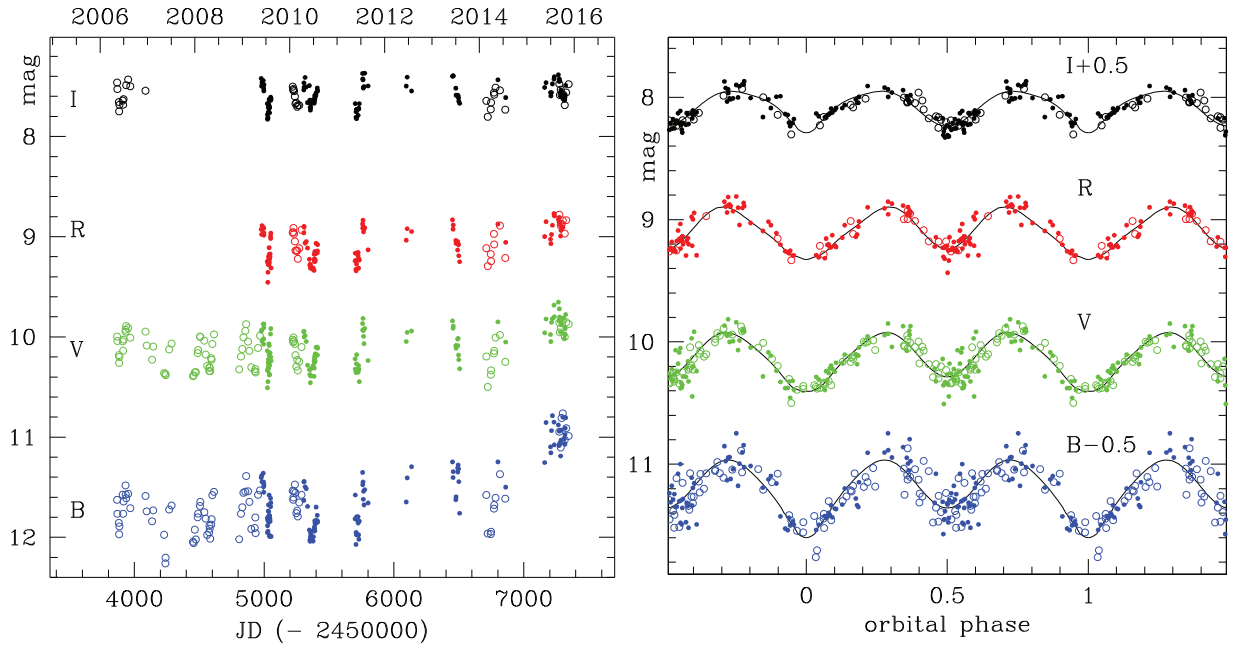


Fig. 1. *Left:* the 2006–2015 BVR_{CLC} lightcurves of T CrB based on our data in Table 1 (solid and open circles mark observations obtained with ANS Collaboration telescopes 11 and 36, respectively). The surge in brightness during 2015 is prominent. *Right:* the quiescence part of the data at left is here phase plotted against the $P=227.55$ days orbital period. The curves are low order Legendre polynomials, symmetric with respect to the WD transit at lower conjunction (phase 0.5), to provide a simple fit to guide the eye to the ellipsoidal modulation.

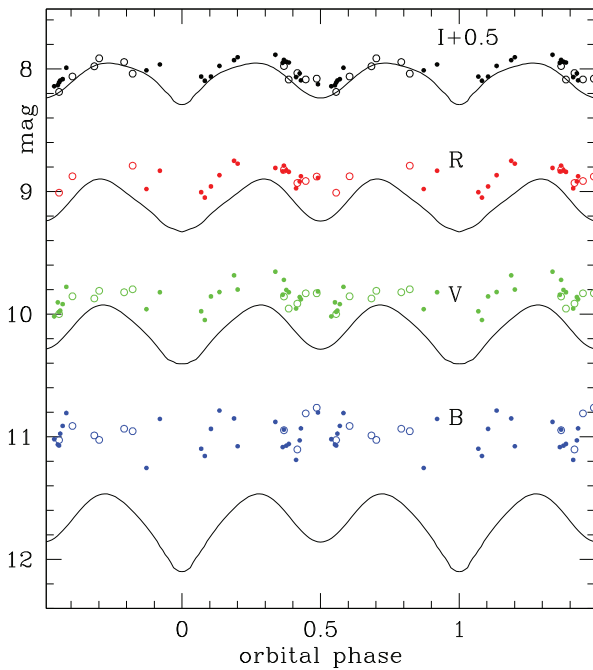


Fig. 2. The photometric observations of T CrB during the 2015 super-active period are phase-plotted against the orbital ephemeris (Eq. (1)), with mean curves for quiescence imported from Fig. 1.

the spectroscopic results from following sections, these photometric signatures are due to: (1) nebular emission from a much larger fraction of the M3III wind now ionized by hot source, which visibility is not affected by orbital motion, and (2) increased irradiation and therefore higher re-emission from the side of the M3III facing the WD. In this respect it is interesting to note that the dispersion of the observations is similar during SACT-2015 and quiescence, with $\sigma(B)=0.115$ and 0.120 mag, respectively. This suggests

that the increased output from the hot source is powered by the same accretion processes and associated instabilities that dominates during quiescence. In addition, the large amplitude and short time scale (of the order of a day or a few days at most) of these erratic fluctuations, suggests that the electron density in the ionized gas (dominating the system brightness in B) is high enough to drive a short recombination time scale, so that the short time scale and large amplitude of the variations in the photo-ionization input are not washed out by reprocessing from the recombining gas.

4. Long term 1947–2015 evolution and previous active states

To place SACT-2015 into a broader perspective, we investigated the long term brightness evolution of T CrB following the 1946 nova outburst. The outburst was over by the summer of 1947 when the star had returned to quiescence brightness, $V \sim 10$ mag. This value is similar to what F. W. A. Argelander measured in 1855 – before the 1866 nova outburst – for his Bonner Durchmusterung (BD) star atlas, and to the brightness that characterized the star in between the two nova eruptions of 1866 and 1946 (Barnard, 1907; Campbell and Shapley, 1923).

To reconstruct the 1947–2015 lightcurve of T CrB, we selected to use the 120,000 visual estimates collected by AAVSO (privately communicated by Stella Kafka, Director). This choice is based on two primary reasons.

The first is that the visual estimates collected by AAVSO constitute an uninterrupted record of T CrB brightness during the last 70 years, whereas other sources of information (measurements in any photometric band) are too sparse in time and scattered through so many different observers, instrumental combinations and photometric systems to be of no use to our goal.

The second argument is based on the fact that during the last 70 years, each epoch has been characterized by a different type of instrument to record stellar brightness: initially unfiltered blue sensitive photographic emulsions, then filtered panchromatic photographic emulsions, followed by photoelectric photometers, and finally by CCD devices. The very red color of T CrB (much redder

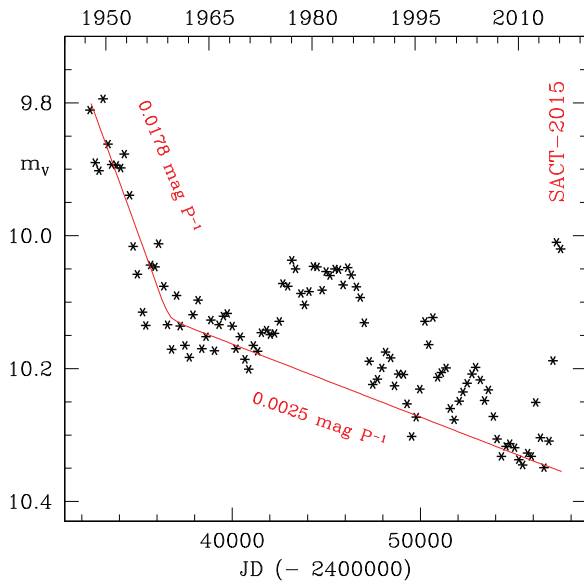


Fig. 3. Long term evolution of the brightness of T CrB in quiescence, from 120,000 AAVSO visual estimates collected after the 1946 nova outburst. Each point represents the mean value of the visual estimates covering an orbital cycle (227.55 days).

than most of the suitable comparison stars around the variable) has impacted in different ways and by different amounts the photometry collected with such a broad assortment of instruments. In addition, only rarely the data have been properly transformed to standard systems, most of the measurements being just differential with respect to a single field star (usually of unmatching colors). On the contrary, visual estimates seem to be far more stable over different epochs and subsequent generations of observers: the comparison sequence has not changed much and the many different observers participating in the 70 years of AAVSO monitoring have used the same measuring device, their unfiltered eyes.

4.1. Mean magnitudes

In tracking the secular evolution of T CrB following the 1946 outburst, we are looking for subtle effects (of the order of hundredths of a magnitude), much less than the scatter intrinsic to visual estimates. We have to filter out the noise.

The simplest way could be to average all data within a given time step. Such a straight average would however most likely generate spurious signals. In fact, the majority of the visual estimates are concentrated during the summer and autumn months, when T CrB is best located in the evening sky. Given the long orbital period of the system (about 62% of 1 year), this would mean that in different years the system is on average observed at different orbital phases. Given the large amplitude of the orbital modulation, this would cause a spurious beating signal.

To overcome the problem, we have divided the AAVSO data into contiguous orbital cycles (110 cycles from 1947 to current time), and χ^2 fitted to them the average phased lightcurve for quiescence (the continuous curve for V band in Fig. 1). In this way, no matter how unevenly distributed in orbital phase the observations could be, a correct estimate for the magnitude averaged along a whole orbital cycle is obtained. The values so derived are plotted in Fig. 3.

4.2. The secular trend and past active phases

The secular trend of T CrB in quiescence, shown in Fig. 3, is characterized by three basic features: (i) an initial faster decline, at a mean rate of 0.0178 mag per orbital period, lasting for the

initial ~ 12 years (1947–1959), (ii) a slower decline, at a mean rate of 0.0025 mag per orbital period, characterizing the following ~ 55 years until present time, and (iii) a few episodes of enhanced brightness occurring after 1975. Four such episodes are clearly present in Fig. 3: the first three occurred in 1975–1985, 1996–1997 and 2001–2004, and were of decreasing peak brightness; the fourth and last one, SACT-2015 is characterized by the largest amplitude with respect the underlying secular trend.

5. Spectroscopy of the 2015 super-active state

In addition to the largest increase in brightness, SACT-2015 has also seen the greatest spectroscopic changes displayed by T CrB since the 1946 nova outburst. The most obvious changes are the unprecedented intensity attained by H ϵ 4686 (in excess of H γ), the large intensity of OIII and NIII lines involved in the Bowen fluorescence mechanism, and the appearance of high ionization lines like [NeV] 3427, all these on top of strong nebular and Balmer continua.

The spectroscopic changes are best illustrated by Fig. 4, where two spectra for exactly the same orbital phase ($\theta=0.53$, WD passing at inferior conjunction) are compared, one from SACT-2015 and the other from the preceding quiescence. The 2015-10-16 spectrum corresponds to the strongest recorded intensity of H ϵ during SACT-2015, while the quiescence 2012-09-03 spectrum is well representative of the usual (and dull) appearance of T CrB during quiescence, when only some weak emission in H α is visible over an otherwise normal M3III absorption spectrum. The result of the subtraction of the quiescence (2012-09-03) from the SACT-2015 spectrum (2015-10-16) is plotted on the lower panel of Fig. 4. It is a fine example of emission from ionized gas of high density (plots built in the same way from other SACT-2015 spectra provide similar results). Integrated flux of the emission lines identified in this nebular spectrum are provided in Table 2.

At the reddest wavelengths, weak features are left in the subtraction of the TiO molecular bands from the two spectra of Fig. 4. To evaluate them, in Fig. 5 we plot template spectra for M2III and M3III giants taken from the atlas of Fluks et al. (1994), after scaling them to the V and $V - I_C$ mean values of T CrB in quiescence at the same orbital phase ($\theta=0.53$). In the same Fig. 5 we plot their difference, which is also over-plotted to the nebular spectrum of Fig. 4, where it provides a perfect match to the weak features left over at reddest wavelengths by the subtraction of the SACT-2015 and quiescence spectra. This indicates that the irradiation by the WD has raised the temperature of the facing side of the giant companion, from that of a M3III during quiescence to that of a M2III during SACT-2015. This change corresponds to an increase in the effective temperature of $\Delta T_{\text{eff}} \sim 80$ K, averaging between $\Delta T_{\text{eff}}=90$ K and $\Delta T_{\text{eff}}=70$ K reported by Ridgway et al. (1980) and Fluks et al. (1994), respectively, as the difference in temperature between M2III and M3III giants.

The intensity of H ϵ has varied considerably during SACT-2015, as illustrated by the sample of spectra presented in Fig. 6. In this figure we also plot for comparison the spectrum for 2014-11-02, that caught T CrB on the transition from quiescence to SACT-2015, which show increased nebular emission (both continuum and lines) and the first appearance of H ϵ . Table 3 lists the integrated flux for a few representative lines as measured on our SACT-2015 low resolution spectra.

6. The nebular spectrum

Some comments are here in order concerning the nebular spectrum of T CrB during SACT-2015, a detailed photo-ionization modeling being pursued elsewhere.

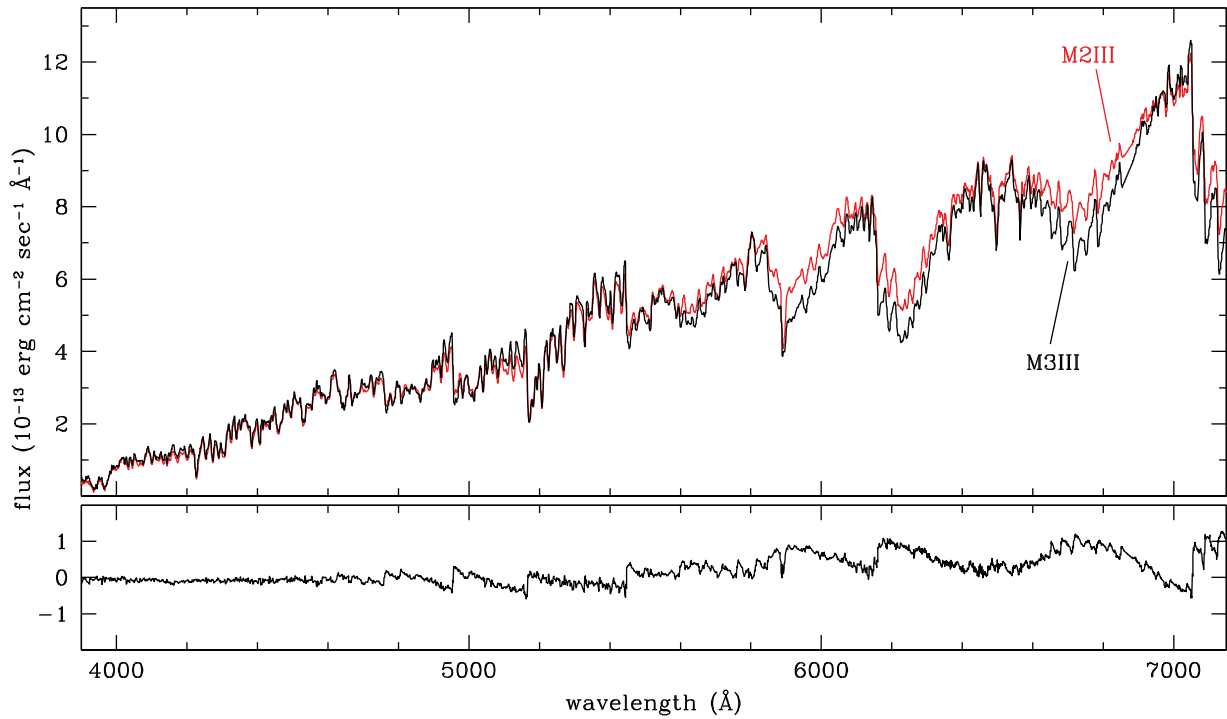


Fig. 5. Spectra for M2III and M3III templates from the atlas of [Fluks et al. \(1994\)](#), and their subtraction, showing the largest difference in the red. (For the interpretation of references to color in this figure legend, the reader is referred to the web version of this article.)

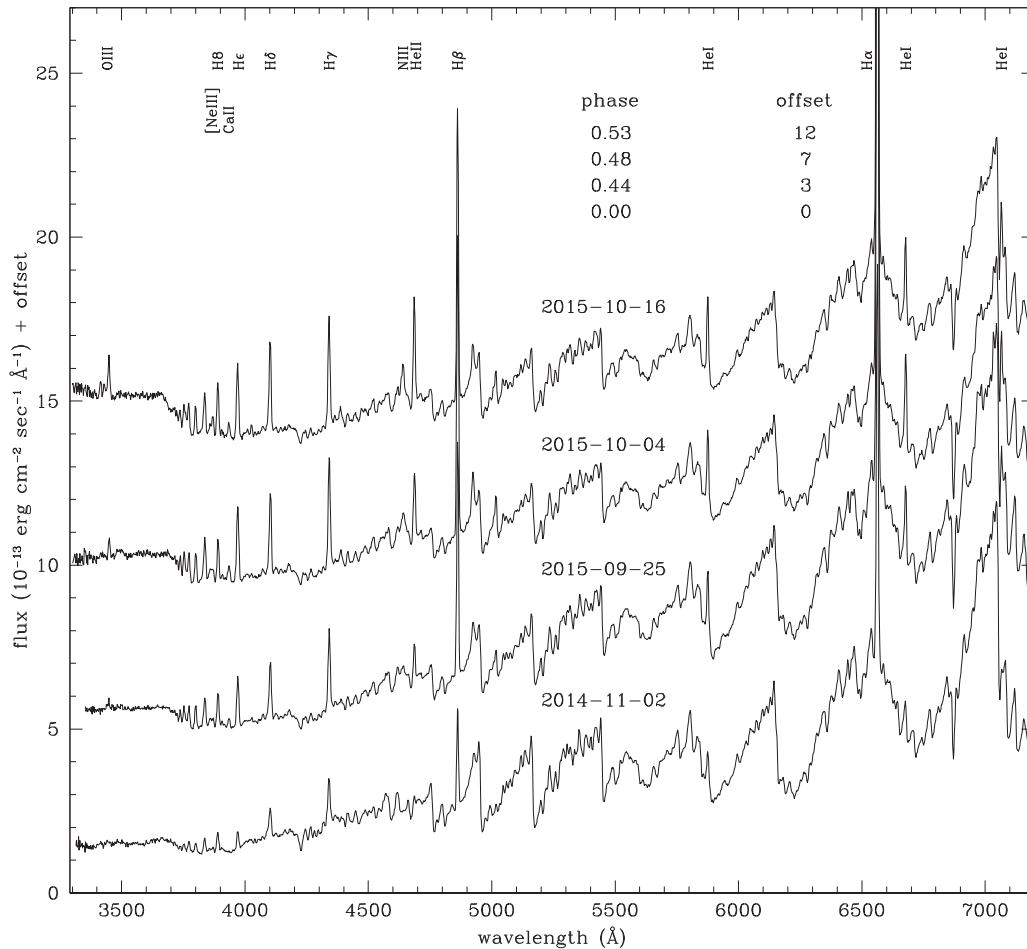


Fig. 6. Sample of low res spectra of T CrB obtained during the 2015 super-active phase, arranged in order of increasing HeII 4686 Å flux.

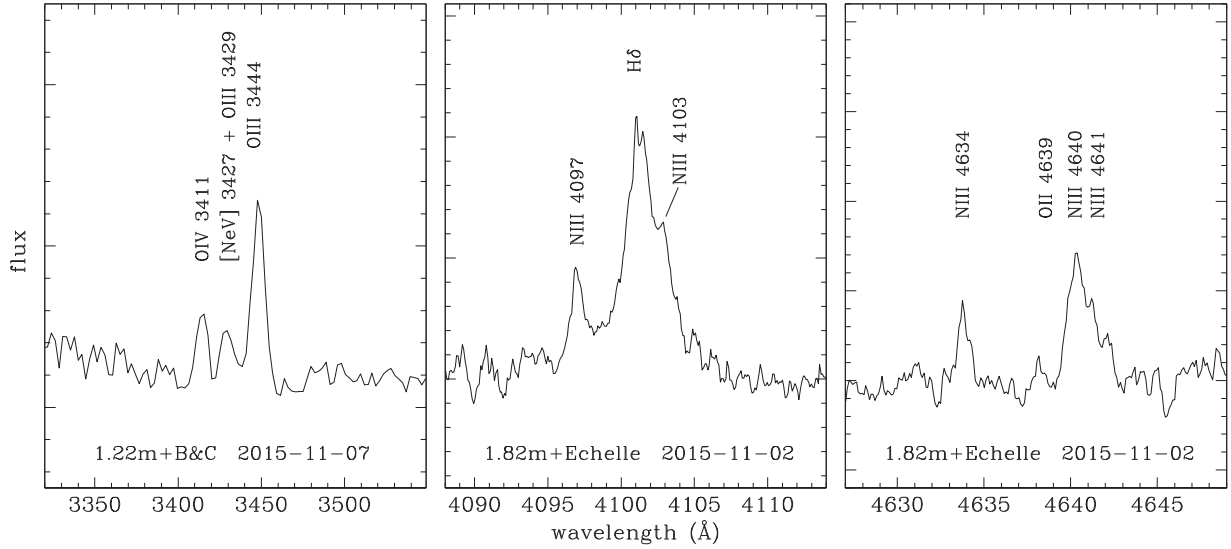


Fig. 7. Zooming on different portions of the spectra of T CrB for the 2015 super-active state, to document the presence of OIV and [NeV] in emission and the main OIII and NIII lines produced by the Bowen fluorescence mechanism.

Table 2

Integrated fluxes (in units of 10^{-13} erg cm^{-2} s^{-1}) of emission lines in the spectrum of T CrB for 2015-10-16 from Fig. 4.

Identification	λ (Å)	Flux
OIV	3411	3.1
[NeV] + OIII	3428	3.5
OIII	3444	10.8
HI + HeI	3733	3.4
HI	3750	5.3
OIII	3758	4.0
HI + HeII	3771	8.3
HI	3797	7.0
HI	3835	11.5
SiII	3859	3.9
[NeIII]	3869	4.8
HI	3888	14.1
CaII	3933	6.6
He ϵ (+[NeIII]+CaII)	3968	24.5
H δ + NIII	4101	25.8
H γ	4340	28.8
HeI	4387	5.4
NIII	4640	25.8
HeII	4686	32.3
HeI	4713	4.7
H β	4861	77.5
HeI	4922	9.2
[OIII]	4959	4.8
[OIII]	5007	18.2
HeI	5016	6.3
HeI	5876	19.6
NaI	5893	3.7
H α	6563	315.0
HeI	6678	17.0
HeI	7065	22.7

Table 3

Integrated fluxes (in units of 10^{-13} erg cm^{-2} s^{-1}) from Asiago 1.22 m+B&C spectra for H α , H β , HeI 5876 Å, and HeII 4686 Å emission lines during the 2015 super-active state of T CrB.

Date	Ph.	H α	H β	HeI	HeII
2014-11-02	0.00	114	27	7	2
2015-06-02	0.94	210	55	17	17
2015-08-11	0.24	242	64	16	18
2015-08-30	0.33	394	93	22	12
2015-09-07	0.36	235	53	12	10
2015-09-24	0.44	319	61	14	9
2015-09-25	0.44	303	64	13	9
2015-10-04	0.48	360	85	17	18
2015-10-16	0.53	330	76	20	28
2015-11-07	0.63	234	76	16	22
2015-11-24	0.71	234	43	13	9
2015-12-23	0.83	244	53	17	20

Fig. 7. The line is observed at 3428 Å, at the mean position for [NeV] 3427 and OIII 3429, which contributes equal amounts to the observed flux. In fact, from Table 2, the observed flux for the 3428 blend is 1/3 of OIII 3444, while that expected from OIII 3429 alone would be 1/6.5, according to both theoretical transition probabilities and actual observations in symbiotic binaries (Selvelli et al., 2007).

The simultaneous presence of both [NeV] 3427 and [NeIII] 3869 could suggest that [NeIV] lines should be equally present in the

nebular spectrum of T CrB. The strongest optical [NeIV] lines are located at 4715–4727 Å (Merrill, 1956), and they never attend a significant intensity (when seen in symbiotic binaries, they score only a few % of the intensity of [NeV] and [NeIII] lines; cf. Allen, 1983, Munari and Zwitter, 2002). The non-detection of [NeIV] in the spectra of T CrB is therefore not surprising. Similarly, the strongest OIV line that is observed at optical wavelengths is the 3411 Å (Jaschek and Jaschek, 2009), and given its modest intensity in the spectra of T CrB no further lines from this ion are expected to be visible.

The relative intensity of HeI and HeII emission lines varied greatly during SACT-2015, as illustrated by the sample of spectra plotted in Fig. 6 and the line fluxes listed in Table 3. The HeII 4686 / (HeI 5876 + HeI 6678) ratio is seen to vary from 0.17 on 2014-11-02, to 0.34 on 2015-08-30, to 0.88 on 2015-10-16. For the latter two dates, the HeI lines augment their intensity by just 20% while HeII increases by three times. This behavior indicates that during quiescence and the initial rise toward SACT-2015, the nebula was *ionization bounded*, with properly nested Stromgren's spheres for different ions and neutral material further out, ready to be ionized by an increase in the hot source output. During SACT, the nebula became *density bounded*, i.e. all the available gas was already ionized and any increase in the hot source output could only rise the ionization degree of the gas but not further expand the nebula

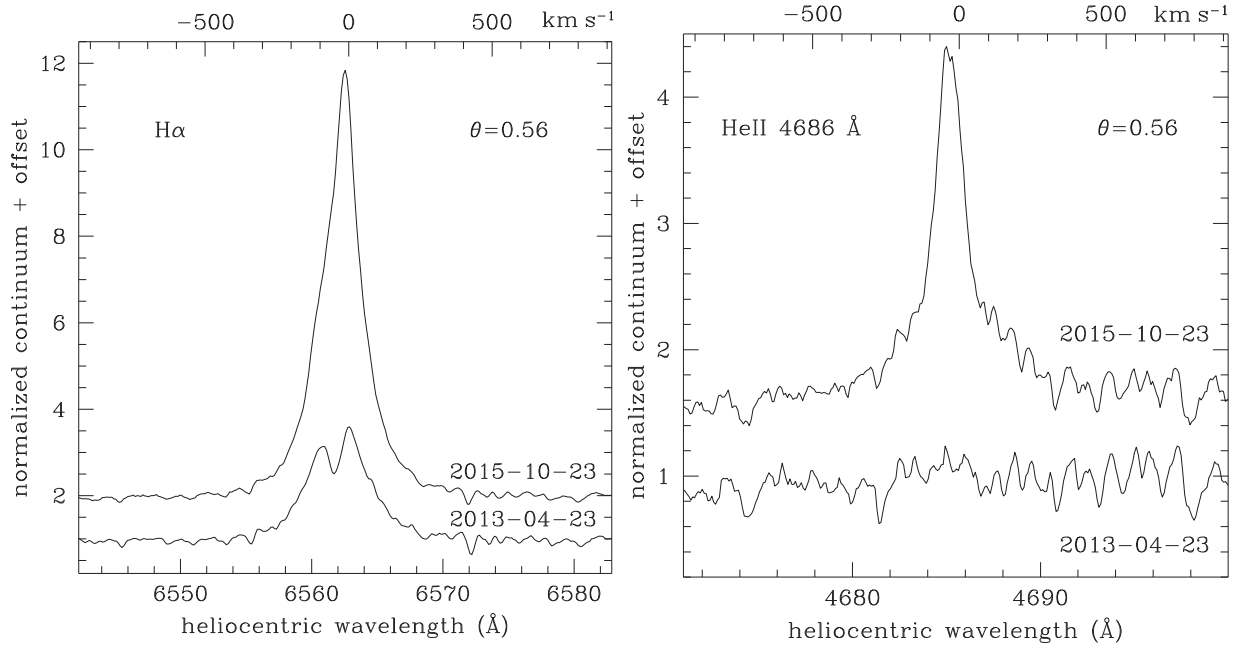


Fig. 8. Comparison of the spectral appearance of T CrB around H α and HeII 4686 Å during quiescence and 2015 super-active state. Asiago 1.82 m+Echelle spectra are compared for exactly the same orbital phase (0.56), to cancel out any dependence from orbital aspect.

into pre-existing external neutral material. The ionization to density bounded transition is nicely confirmed by the evolution of the H α profiles shown in Fig. 8, where a quiescence (2013-04-23) and a SACT-2015 (2015-10-26) profile for exactly the same orbital phase (0.56) are compared. The H α profile for quiescence shows a weak emission and superimposed to it a narrow absorption, which is missing from the SACT-2015 profile that displays a vastly stronger emission. This narrow absorption is typical of symbiotic stars, and originates in the outflowing wind of the cool giant, specifically from the neutral portion external to the fraction ionized by the WD, as it was demonstrated by Munari (1993) who followed for several cycles the orbital motion of the cool giant, of the emission lines and of the narrow absorptions in EG And, a symbiotic star with optical spectra closely similar to those of T CrB in quiescence. The absence of the narrow central absorption from the SACT-2015 profile indicate that, in the direction of the observer, no neutral gas exists external to the ionized gas. The velocity of the narrow absorption is -19 km s^{-1} with respect to that of the cool giant, which is therefore the terminal velocity of its outflowing wind, a value typical of cool giants.

Finally, the values reported in Table 3 shows how the intensity of HeII 4686 emission line is more responsive to the varying activity of the hot source than to the orbital aspect.

7. Three levels of activity for T CrB in quiescence

Iijima (1990) noted that during quiescence, i.e. away from the 1866 and 1946 nova outbursts, T CrB exhibits two states: an “high” one when emission lines (Balmer, HeI) and the nebular continuum are relatively strong, and a “low” state when they essentially disappear (except some weak residual emission in H α). The unique conditions experienced by T CrB during SACT-2015 requires the introduction of a new, third state that we term “super-active”, which is characterized by (1) the presence of OIV and [NeV] lines, a very strong HeII 4686, and a strong 4640 Bowen fluorescence blend, (2) a large increase in mean brightness, and (3) disappearance of orbital modulation from B-band lightcurve.

We have searched the available literature (e.g. Kraft, 1958; Gravina, 1981; Andriolat and Houziaux, 1982; Blair et al., 1983; Williams, 1983; Kenyon and Garcia, 1986; Iijima, 1990; Anupama and Prabhu, 1991; Ivison et al., 1994; Anupama, 1997; Zamanov and Marti, 2001; Munari and Zwitter, 2002) in the attempt to reconstruct the history of spectroscopic activity of T CrB during quiescence. This has turned out a difficult task because rarely integrated absolute fluxes are provided for the emission lines, few observations ventured enough into the blue to cover the Balmer continuum, and usually only equivalent widths are given if not just a mere description like ‘weak’ or ‘strong’. In addition the observations reported in literature were obtained at different wavelength intervals and resolving powers. We tried our best to homogenize the different sources, and in this we took advantage of the many (unpublished) spectra of T CrB that we have regularly obtained since 1987.

T CrB has always been in a ‘low’ state when observed for the first 3 decades after the 1946 outburst. The last of these spectra, those of Blair et al. (1983) for 1981-02-06, Williams (1983) for 1981-06-10, and Gravina (1981) for 1981-07-15 and 1981-09-15 record only feeble emission in H α , H β and H γ . Iijima (1990) reports that, in addition to Balmer and HeI, a weak emission in HeII 4686 Å was visible on his spectra on several dates distributed between 1982 and 1987, but Kenyon and Garcia (1986) saw no HeII in emission on their 1984 and 1985 spectra and the absolute flux they measured for Balmer lines was only twice larger than that reported by Blair et al. (1983) for 1981. The extensive spectral monitoring by Anupama and Prabhu (1991) and Anupama (1997) shows that the intensity of Balmer and HeI emission lines gradually increased starting with June 1985, peaked during November 1986, and returned to the ‘low’ state by October 1987, where T CrB has remained until 1996. Iijima (1990) confirms that HeII was absent from his spectra for 1988, 1989 and 1990, the same reported by Ivison et al. (1994) for their 1989 spectra. Just a feeble emission in the lower Balmer lines and no HeII were found by Munari and Zwitter (2002) on various dates of 1993 and 1995. Then a new ‘high’ state was briefly observed in 1996–1997. On 1996-02-01 Zamanov and Marti (2001) found H α to be weak and this is

confirmed by a 1996-02-08 spectrum from [Munari and Zwitter \(2002\)](#) that in addition reveals Hell to be absent. Then, [Mikolajewski et al. \(1997\)](#) found H α to be in strong emission during April, May and June of 1996. This is confirmed by a 1996-05-30 spectrum from [Munari and Zwitter \(2002\)](#), that in addition shows how Hell was still absent. [Zamanov and Marti \(2001\)](#) reports that by 1998 this second 'high' state of T CrB was over. Since then and to the best of our knowledge, T CrB has never been observed again in a 'high' state until the 2015 episode described in this paper. The long term photometric behavior presented in [Fig. 3](#) shows that T CrB rised significantly above the underlying secular decline only in correspondence of the high spectroscopic states.

To the best of our knowledge, T CrB has been caught in a super-active state in only one other occasion, on the summer of 1938 by [Hachenberg and Wellmann \(1939\)](#). On their spectrum for 22 July 1938, Hell 4686 is half the intensity of H γ and the 4640 Å blend stands in prominent emission (2/3 the intensity of Hell). The [Hachenberg and Wellmann \(1939\)](#) spectrum for August 28 confirms the super-active state, while that for September 22 indicates a rapid return of T CrB toward lower excitation conditions.

There is an intriguing parallelism between SACT-2015 and what [Hachenberg and Wellmann \(1939\)](#) observed in 1938. The super-active state they caught occurred ~ 70 years past the 1866 nova outburst, and SACT-2015 is occurring ~ 70 years past the 1946 nova outburst. Is therefore everything in place for a new nova outburst in 2026, again ~ 80 years past the last eruption?

References

- Allen, D.A., 1983. MNRAS 204, 113.
 Allen, D.A., 1984. PASAu 5, 369.
 Andriillat, Y., Houziaux, L., 1982. In: Fridjung, M., Viotti, R. (Eds.), The nature of symbiotic stars. Reidel ASSL 95, p. 57.
 Anupama, G.C., 1997. In: Mikolajewska, J. (Ed.), Physical processes in symbiotic binaries and related systems, vol. 117. Copernicus Foundation for Polish Astronomy.
 Anupama, G.C., Prabhu, T.P., 1991. MNRAS 253, 605.
 Bailey, J., 1975. JBAA 85, 217.
 Barker, T., 1978. ApJ 219, 914.
 Barnard, E.E., 1907. ApJ 25, 279.
 Belczynski, K., Mikolajewska, J., 1998. MNRAS 296, 77.
 Blair, W.P., Feibelman, W.A., Michalitsianos, A.G., Stencel, R.E., 1983. ApJS 53, 573.
 Bowen, I.S., 1934. PASP 46, 146.
 Bowen, I.S., 1935. ApJ 81, 1.
 Campbell, L., Shapley, H., 1923. HarCi 247, 1.
 Cannizzo, J.K., Kenyon, S.J., 1992. ApJ 386, L17.
 Cassatella, A., Patriarchi, P., Selvelli, P.L., Bianchi, L., Cacciari, C., Heck, A., Peryman, M., Wamsteker, W., 1982. ESASP 176, 229.
 Dobrotka, A., Hric, L., Casares, J., Shahbaz, T., Martínez-Pais, I.G., Muñoz-Darias, T., 2010. MNRAS 402, 2567.
 Eriksson, M., Johansson, S., Wahlgren, G.M., Veenhuizen, H., Munari, U., Siviero, A., 2005. A&A 434, 397.
 Feibelman, W.A., 1983. ApJ 275, 628.
 Fekel, F.C., Joyce, R.R., Hinkle, K.H., Skrutskie, M.F., 2000. AJ 119, 1375.
 Fluks, M.A., Plez, B., The, P.S., de Winter, D., Westerlund, B.E., Steenman, H.C., 1994. A&AS 105, 311.
 Gravina, R., 1981. IBVS 2041, 1.
 Gromadzki, M., Mikolajewski, M., Tomov, T., Bellas-Velidis, I., Dapergolas, A., Galan, C., 2006. A&A 56, 97.
 Hachenberg, O., Wellmann, P., 1939. ZA 17, 246.
 Harrington, J.P., 1972. ApJ 176, 127.
 Henden, A., Munari, U., 2006. A&A 458, 339.
 Iijima, T., 1990. JAVSO 19, 28.
 Ivison, R.J., Bode, M.F., Meaburn, J., 1994. A&AS 103, 201.
 Jaschek, C., Jaschek, M., 2009. The Behavior of Chemical Elements in Stars. Cambridge University Press.
 Kenyon, S.J., 1986. The Symbiotic Stars. Cambridge University Press.
 Kenyon, S.J., Garcia, M.R., 1986. AJ 91, 125.
 Kraft, R.P., 1958. ApJ 127, 625.
 Merrill, P.W., 1956. Lines of the Chemical Elements in Astronomical Spectra. Carnegie Institution of Washington Publication, p. 610.
 Mikolajewski, M., Tomov, T., Kolev, D., 1997. IBVS 4428, 1.
 Munari, U., 1993. A&A 273, 425.
 Munari, U., 1997. In: Mikolajewska, J. (Ed.), Physical Processes in Symbiotic Binaries and Related Systems. Copernicus Foundation for Polish Astronomy, p. 37.
 Munari, U., et al., 2012. BaltA 21, 13.
 Munari, U., et al., 2014. AJ 148, 81.
 Munari, U., Moretti, S., 2012. BaltA 21, 22.
 Munari, U., Zwitter, T., 2002. A&A 383, 188.
 Paine-Gaposchkin, C.H., 1957. The Galactic Novae. North-Holland Publishing Co.
 Pettit, E., 1946. PASP 58, 153.
 Ridgway, S.T., Joyce, R.R., White, N.M., Wing, R.F., 1980. ApJ 235, 126.
 Ruffert, M., Cannizzo, J.K., Kenyon, S.J., 1993. ApJ 419, 780.
 Sanford, R.F., 1946. PASP 58, 240.
 Sanford, R.F., 1947. PASP 59, 87.
 Sanford, R.F., 1949. ApJ 109, 81.
 Schaefer, B.E., 2010. ApJS 187, 275.
 Schlafly, E.F., Finkbeiner, D.P., 2011. ApJ 737, 103.
 Schlegel, D.J., Finkbeiner, D.P., Davis, M., 1998. ApJ 500, 525.
 Selvelli, P., Danziger, J., Bonifacio, P., 2007. A&A 464, 715.
 Selvelli, P.L., Cassatella, A., Gilmozzi, R., 1992. ApJ 393, 289.
 Skopal, A., 2005. A&A 440, 995.
 Warner, B., 1995. Cataclysmic Variable Stars. Cambridge Astrophysics Series, p. 28.
 Webbink, R.F., 1976. Natur 262, 271.
 Williams, G., 1983. ApJS 53, 523.
 Williams, R.E., 1992. AJ 104, 725.
 Yudin, B., Munari, U., 1993. A&A 270, 165.
 Zamanov, R., Bode, M.F., Stanishev, V., Martí, J., 2004. MNRAS 350, 1477.
 Zamanov, R., Marti, J., 2001. IBVS 5013, 1.
 Zamanov, R.K., Bruch, A., 1998. A&A 338, 988.